Heliyon

Multi-parameter optimization of the capacitance of Carbon Xerogel catalyzed by NaOH for application in supercapacitors and capacitive deionization systems

Mahdi Alam [a],[*]**, Seyed Ahmad Mirbagheri** [a]**, Mohammad Reza Ghaani** [b]

[a] *Department of Civil and Environmental Engineering, K.N. Toosi University of Technology, No. 1346, Vali Asr*
Street, Mirdamad Intersection, Tehran, Iran

[b] *School of Chemical and Bioprocess Engineering, University College Dublin, Belfield, Dublin 4, Ireland*

[*] Corresponding author.
E-mail address: maalam@mail.kntu.ac.ir (M. Alam).

Abstract

Carbon Xerogel is an economic choice of material for electrodes with applications in Electric Double Layer Capacitors (EDLCs) and Capacitive DeIonization systems (CDI, particularly for desalination). The objective here is to optimize Carbon Xerogel's performance, specifically its capacitance, through multi-parameter optimization using Response Surface Methodology (RSM). We choose NaOH as the catalyst and select as the optimization parameters (i) the pH of the initial Resorcinol-Formaldehyde-Catalyst (RFC) solution, (ii) Reactants to Liquid mass ratio (R/L) of the RFC solution, and (iii) the Pyrolysis Temperature (PT). For a selected range of these three parameters, we obtain an optimum capacitance of Carbon Xerogel equal to 37.6 F/g with optimized parameters PT = 800, R/L = 30% and pH = 5.7. Through comparing Carbon Xerogel samples synthesized with Na_2CO_3 versus NaOH as the catalyst, we show that the capacitance not only depends on the pH of the initial RFC solution, but also is a strong function of the catalyst material.

1. Introduction

Materials with high specific capacitance are critical elements in the fabrication of electrodes for Electric Double Layer Capacitors (aka EDLCs or Supercapacitors) and Capacitive DeIonization (CDI) systems. Supercapacitors are needed when energy is to be stored and released very rapidly. They can manage a much higher power rates than chemical batteries and therefore, while they may have a limited storage capacity, are ideal for applications in which a sudden power surge is needed [1, 2]. Capacitive DeIonization (CDI) system, also has received a great deal of attention in recent years mostly for its application in desalination of brackish and saline water and also some water purifications like dye removals [3]. The CDI has an adsorption mechanism similar to Electric Double Layer Capacitors (EDLCs) [4].

Electrode performance in these applications not only depends on specific capacitance, but also on other factors such as high specific surface area, pore metrics, electrochemical cyclic stability, electrical conductivity, and materials fabrication cost of electrodes [5, 6, 7, 8]. Different porous carbon based materials are extensively used as the electrode in supercapacitors and CDI systems. Examples of such carbon materials are Activated Carbon (AC), Carbon Aerogels (CA), Carbon Nano Tubes (CNT), Carbon Nano Fibers (CNF) and Graphene [2, 4, 5, 6, 9, 10]. Among these, Carbon Aerogel is one of the most widely used material for electrodes because of its high mass-specific surface area, low resistivity, high electrical conductivity, environmental compatibility and chemical stability [11]. Carbon gels are consistently prepared through a sol-gel polycondensation of Resorcinol with Formaldehyde by adding a catalyst. The main advantage of these carbon material is that its pore metrics can be modified by using an easy to implement sole-gel technique [12].

Carbon gels are categorized based on the drying method used to extract water from the initial gel structure. The way water is extracted and the rate of extraction, play a vital role in the porosity volume, the type of the pores and specific surface area, and therefore the capacitance of the final product. Common drying methods are supercritical drying, freeze drying, and ambient pressure drying. The final dried gel obtained through each of these drying methods is, respectively, called Carbon Aerogel, Carbon Cryogel and Carbon Xerogel [13]. Since Carbon Xerogel is dried in the ambient pressure and temperature, contrary to other two carbon gels, does not require specific and expensive drying equipment and therefore is much more economic. This reduction in cost comes at the expense of reduced porosity, specific surface area and the overall capacitance. The goal here, is to increase the quality of Carbon Xerogel (specifically the capacitance) while maintaining the simplicity and cost efficiency of the production process.

One of the most important factors in the synthesizing of the Carbon Xerogel is the type and amount of catalyst used in the production process [14, 15, 16]. Carbon Xerogel is typically produced with the use of different catalysts such as Na_2CO_3, NaOH, $Ca(OH_2)$, K_2CO_3 and Acetic acid [13, 16]. It is to be noted that if these compounds act as the corrosive material that partially dissolves solid carbon-based composite (e.g. biomass) before the heat treatment process, they are typically called activating agents [17, 18]. Otherwise, if we use them as the precursor to adjust the solution acidity and facilitate the polymerization reaction, they are called catalysts, which is the case in this manuscript.

Here, we optimize the obtainable capacitance of prepared Carbon Xerogel catalyzed by NaOH. In order to do so, we study the effect of (i) pH of the initial Resorcinol-Formaldehyde-Catalyst (RFC) solution, (ii). Reactants to Liquid mass ratio (R/L), and (iii) Pyrolysis Temperature (PT) on the density and the capacitance of the final synthesized Carbon Xerogel. Capacitance is clearly one of the objectives, and density of the final gel is a measure of porosity and affects "scalability" of the final electrode: if porosity is higher, then ions will have a better accessibility to adsorption surfaces, and therefore we can make a thicker electrode with a higher ion adsorption capacity. To find the desired optimum Carbon Xerogel, we perform optimization on the three aforementioned parameters (pH, R/L, PT) through the Response Surface Methodology (RSM).

It is believed by some researchers that it is the final pH of the RFC solution (produced by the catalyst) that affects the capacitance of the synthesized electrode, and not the catalyst type and amount [19, 20]. Here, to investigate this issue, we consider two different catalysts (Na_2CO_3 and NaOH) to synthesize Carbon Xerogel and show that with the same pH of RFC solutions (keeping all other parameters the same), these two electrodes have difference capacitance values, and therefore the type of the catalyst is, in fact, important.

This article is consists of four following parts: the materials we used to synthesize our Carbon Xerogel samples and the method of synthesizing are provided in section 2. We also introduce our methodology for optimization of the electrode properties in this section. The results of optimizations and the equations obtained from RSM are presented and discussed in section 3. We conclude the paper in section 4.

2. Materials and methods

2.1. Carbon Xerogel synthesized method

In order to synthesize Carbon Xerogel, we add Resorcinol (99%, Merck KGaA, Germany) with the 2:1 molar ratio to the Formaldehyde solution (37%, Merck KGaA, Germany). We then mix the two with a magnetic stirrer and add the catalyst to speed

up the interconnectivity of the primary particles. The amount of the catalyst are measured, in most studies, with the Resorcinol to Catalyst molar ratio (R/C) with a wide range varying from 50 to more than 3000 [21, 22, 23, 24, 25, 26]. In some studies, this amount is measured based on the pH of the initial Resorcinol-Formaldehyde-Catalyst (RFC) solution [19, 20]. Since our objective is to investigate the effect of the type and the amount of the catalyst on the final capacitance of our synthesized Carbon Xerogel sample, we use the latter method of measurement based on pH and compare the results for two different types of catalysts: NaOH and Na_2CO_3.

To synthesize the initial Carbon gel, the obtained RFC solution must be treated thermally (the so-called gelation stage). There are various proposed timing and temperature range for this stage, but common among all is that temperature rises gradually from the room to the gelation temperature. The RFC solution is then kept under the constant gelation temperature for 2−5 days for the gel to fully form. Here, we follow Saliger et al [27] and keep the RFC solution at the room temperature for 24 hours, followed by another 24 hours at 50 °C, and finally for 72 hours at 90 °C.

The next step is to remove liquid from the structure (the drying stage). This is a very important stage in the synthesizing of the Carbon gel because porosity, size of the pores, specific surface area, and capacitance of the final sample are highly sensitive to how water is extracted from the initial gel. A major challenge here is the fact that the surface tension upon evaporation can break the Carbon gel structure. This can result in a major shrinkage of the gel and hence can significantly affect (negatively) desired properties of our Carbon gel. This has inspired variety of drying methods. The most important and widely used drying methods that have minimum negative impact on aforementioned desired properties are supercritical drying [28, 29, 30, 31, 32] and freeze drying [21, 30, 33, 34]. The resulting Carbon gel from each method is called, respectively, a Carbon Aerogel and a Carbon Cryogel. Both supercritical and freeze drying methods need specialized and expensive apparatus. This has motivated an extensive research on the (cheaper and simpler) ambient-pressure drying method whose outcome is called Carbon Xerogel. Clearly, the reduced cost and complexity comes at the expense of reduced quality of the final Carbon gel.

In an ambient-pressure drying method, the water is usually exchanged with another liquid with a lower surface tension, such as Acetone. To do so, the wet Carbon gel is submerged in an Acetone container for 24 hours. During this period, Acetone in the container is changed with pure Acetone at least two times. This is to make sure that Acetone has fully replaced all water particles in the Carbon gel structure. We then place the wet Carbon gel at the ambient pressure and temperature for 24 hours for the Acetone particles to evaporate. It is important that the evaporation occur at a gradual pace, and therefore we put the sample inside a container with a small outlet to the air in order to control the rate of evaporation.

The final stage of Carbon Xerogel synthesis is the so-called Pyrolysis. In this stage, the dried Carbon gel is put inside a controlled atmosphere heat treatment furnace at the Pyrolysis temperature. We use Argon as the flowing gas in order to prevent oxidation and burning of the Carbon. Suggested Pyrolysis temperature and duration is respectively from 600 °C to 1200 °C and from 1 to 5 hours [13, 35, 36, 37, 38, 39]. We set the Pyrolysis time to 3 hours, and the varied the temperature from 600 °C to 900 °C. To avoid temperature shock to our sample, the furnace temperature is first gradually raised from the ambient temperature (25 °C) to 300 °C over a 30-minute period, and then to 600 °C over an additional 45-minute. For the tests that require Pyrolysis temperatures higher than 600 °C, the increase rate in the temperature beyond 600 °C is set at 5°C/minute. Finally, the Carbon gel is kept at the desired temperature of the test for 3 hours. The flow of the Argon continues until our gel is cooled down.

2.2. Parameters affecting Carbon Xerogel characteristics

There are several parameters that can be tuned during the synthesis of Carbon Xerogel. Some of which can significantly affect the quality of the final gel. These include Resorcinol to Formaldehyde molar ratio, catalyst type, Resorcinol to Catalyst molar ratio (R/C), pH of the initial RFC solution, reactant to liquid mass ratio, gelation time, gelation temperature, drying method, solvent exchanging, pyrolysis temperature, and the pyrolysis time. Past studies have shown that considerable impact on the final gel properties mainly comes from the pH of the initial RFC solution, reactant to liquid ratio, and pyrolysis temperature [8, 13, 16, 19, 22, 23, 40]. Therefore, in this study, we consider these three parameters within the range that is widely used in the literature (see Table 1).

2.3. Experimental design for Response Surface Methodology (RSM)

The RSM method requires a set of experimental data to obtain an optimum full-quadratic model. There are different "experiment design" methodologies proposed

Table 1. Main parameters affecting the properties of synthesized Carbon Xerogel.

Variables	Symbol	Experimental range	
		Coded values	Actual values
pH of initial RFC solution[a]	pH	−1, 0, 1	5.5, 6.25, 7.0
Reactant to liquid mass ratio (%)	R/L	−1, 0, 1	30, 40, 50
Pyrolysis temperature (°C)	PT	−1, 0, 1	600, 750, 900

[a] RFC solution: Resorcinol-Formaldehyde-Catalyst solution.

for RSM, among which, Box-Behnken Design (BBD) is more suitable for our purpose that has a limited range of parameter variations. We consider three levels of each of relevant parameters (i.e. pH, R/L and PT) in actual and coded values (Table 1), and the BBD (with three centerpoint runs) gives us a set of 15 required experiments (Table 2, first eight columns from left). Once results of these experiments are at hand, RMS gives the following full quadratic model (Eq. (1))

$$Y = \beta_0 + \sum_{i=1}^{k} \beta_i X_i + \sum_{i=1}^{k} \beta_{ii} X_i^2 + \sum_{i=1}^{k-1} \sum_{j=i+1}^{k} \beta_{ij} X_i X_j + \varepsilon, \tag{1}$$

in which k is the number of variables (here k = 3), β_0 intercept constant or constant term of the equation, X_i independent variables (i.e. our parameters), Y is the response (here the density and the capacitance), β_i, β_{ii} and β_{ij} are respectively coefficients of linear, quadratic and interaction parameters, and ε is the residual associate to the experiment. This model gives us a quantitative insight on the effect of each variable and their mutual interactions on the target response.

Table 2. Set of experiments in coded and actual values format based on Box-Behnken design.

Standard order	Run order	Variables						Responses	
		X1		X2		X3		Y1	Y2
		pH		R/L		PT		Density	Capacitance
		Coded	Actual value	Coded	Actual value	Coded	Actual value	g/cm^3	F/g
14	1	0	6.25	0	40	0	750	0.529	30.39
5	2	−1	5.50	0	40	−1	600	0.602	0.62
2	3	1	7.00	−1	30	0	750	0.958	12.19
3	4	−1	5.50	1	50	0	750	0.750	22.44
6	5	1	7.00	0	40	−1	600	0.989	4.78
9	6	0	6.25	−1	30	−1	600	0.437	9.09
13	7	0	6.25	0	40	0	750	0.552	31.04
8	8	1	7.00	0	40	1	900	1.245	3.83
15	9	0	6.25	0	40	0	750	0.483	34.96
10	10	0	6.25	1	50	−1	600	0.757	13.35
12	11	0	6.25	1	50	1	900	0.819	21.79
7	12	−1	5.50	0	40	1	900	0.629	25.13
4	13	1	7.00	1	50	0	750	0.796	29.45
1	14	−1	5.50	−1	30	0	750	0.255	31.63
11	15	0	6.25	−1	30	1	900	0.552	20.63

2.4. Evaluation of electrochemical properties of synthesized electrode

Capacitance of a sample is an important measure of its electrochemical properties. There are different methods to experimentally measure the capacitance of an electrode, e.g. Cyclic Voltammetry (CV), Electrochemical Impedance Electroscopy (EIS) and Chronopotentiometry [41, 42, 43, 44]. Here, we use Cyclic Voltammetry as is commonly used by many researchers [8, 25, 45, 46, 47, 48, 49].

In three-electrode Cyclic Voltammetry (CV) a voltage is established between a working electrode (here our Carbon Xerogel electrode) and a reference electrode. The current is then measured by a third electrode, which is called the counter electrode. The capacitance is then determined via Eq. (2):

$$C = \frac{1}{2\Delta V}(Q_a + Q_c), \tag{2}$$

where ΔV is the voltage range in the CV test, and Q_a and Q_c are respectively anodic and cathodic electrode charges given by Eq. (3):

$$Q = \int I \, dt = \int \left[I(v)dv \times \frac{dt}{dv} \right] = \frac{\int I(v)dv}{\frac{dv}{dt}} = \frac{\int I(v)dv}{r}, \tag{3}$$

in which I is the measured current and $r = \frac{dv}{dt}$ is the voltage scan rate. Note that $\int I(v)dv$ is the area under the current vs voltage curve, which is called the CV curve. In order to be able to compare capacitance of different electrodes we need to normalize the capacitance of each electrode to its mass (m). The outcome is called *mass specific capacitance* or in brief *specific capacitance* (Eq. (4)).

$$C = \frac{\int I(v)dv}{2mr\Delta V}. \tag{4}$$

Here, we use a potentiostat (μAutolabIII, Metrohm, Netherland) for our cyclic voltammetry tests with a Platinum wire as the counter electrode. We measure the Capacitance within the potential range of $-0.4-0.6$ V (vs Ag/AgCl) at the scan rate of 10 mV/s in 0.5M NaCl aqueous solution as the electrolyte.

The Scanning Electron Microscope (SEM) images are also used to visualize the morphology of synthesized electrodes, and to evaluate the effect of pore size and distribution on the final capacitance.

2.5. pH adjustment of the initial RFC solution

As discussed before, one of the three major parameters affecting the electrode properties is the pH of the initial RFC solution. When Resorcinol is added to a 37%

Formaldehyde solution with a 2:1 molar ratio, the pH of the obtained solution is in the range of 3.6–3.9 according to different Reactant to Liquid ratios (R/L). This pH is increased (i.e. acidity decreases) when a alkaline catalyst is added to the solution. Since the volume of our initial RFC sample is small (20 ml), adding even a miniscule of catalyst can result in a dramatic change in the pH and therefore targeting a specific pH will be very difficult. To address this issue we add different volumes of diluted catalyst solution (0.03M) to our Resorcinol-Formaldehyde solution and measure the pH. We then plot the final pH versus the volume of the diluted catalyst solution (the so-called *a pH standard curve*). Using these curves, we can find precisely the required volume of the catalyst solution to obtain a specific pH.

3. Results and discussion

3.1. pH standard curves

Results of our experiment quantify the variation of the pH of the initial RFC solution as a function of the volume of 0.03M catalyst solution for different R/L ratios, as is shown in Fig. 1. From the curves of Fig. 1 (the pH standard curves) one can determine the required NaOH catalyst solution for obtaining a specific desired pH.

Here, we would like to comment that some prior studies have used R/C ratio as a measure of amount of the catalyst [21, 22, 23, 24, 25, 26]. However, it is important to note that when dealing with different catalysts in preparing of the initial RFC solution, the relationship between the R/C ratio and the pH of the solution are different depending on the catalyst type. We show this relationship between pH and amount of the catalyst (mmole) for different catalysts (NaOH and Na_2CO_3) and different R/L ratios (R/L = 0.3, 0.4, and 0.5) in Fig. 2. In some cases, the difference in the pH due
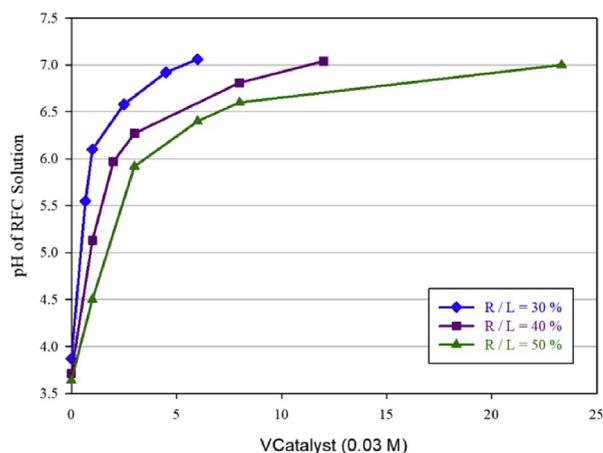

Fig. 1. pH standard curves for calculating the amount of catalyst (NaOH 0.03 M) needed to achieve the desired pH for initial RFC solution.
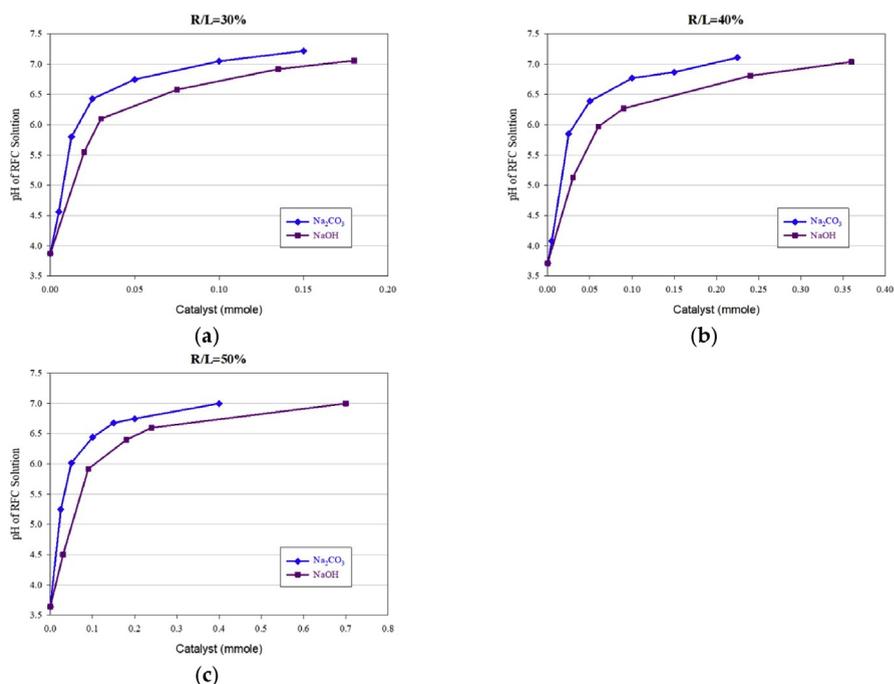
Fig. 2. pH comparison of RFC solution with NaOH vs Na$_2$CO$_3$ catalyst: (a) R/L = 30%; (b) R/L = 40%; (c) R/L = 50%. (Equal R/C ratio for different catalysts results different pH, therefore if the pH of initial RFC solution is the main affecting parameter, using R/C ratio is not a proper choice).

to the same amount of catalyst can be as large as 15 percent (see Fig. 1(c) for R/L = 50% & C = 0.03 mmole, pH = 4.5 & 5.25 for different catalysts).

3.2. Density minimization of Carbon Xerogel using Response Surface Methodology (RSM)

We conduct the required 15 experiments as designed by BBD method, and as the first response measure the density of final samples. Using RSM, we can then fit the optimum 2nd order algebraic equation to our results. The resulted equations for the coded and actual value of variables are presented respectively in Eqs. (5) and (6).

$$
\ln(Y) = -0.6523 + 0.3202X_1 + 0.2299X_2 + 0.0735X_3 + 0.2276X_1^2 - 0.0566X_2^2 \\
+ 0.2339X_3^2 - 0.3161X_1X_2,
$$

(5)

$$
\ln(\text{Density}) = 5.60 - 2.944\,\text{pH} + 0.3317\,\text{R/L} - 0.0151\,\text{PT} + 0.4046\,\text{pH}^2 \\
- 0.000566\,(\text{R/L})^2 + 0.000010\,\text{PT}^2 - 0.04214\,\text{pH} \times \text{R/L}.
$$

(6)

To find the fitting quality of the above equations, we first consider the ANalysis Of VAriance (ANOVA) table. It turns out, as is shown in Table 3, that the P-value of

Table 3. ANOVA table of RSM represented model for Density.

Source	DF[a]	Adj SS[b]	Adj MS[c]	F-value	P-value
Model	7	2.08106	0.297294	69.95	<0.001
Linear	3	1.28643	0.428811	100.89	<0.001
pH	1	0.82044	0.820441	193.03	<0.001
R/L	1	0.4228	0.422798	99.47	<0.001
PT	1	0.04319	0.043194	10.16	0.015
Square	3	0.39504	0.131682	30.98	<0.001
pH × pH	1	0.19121	0.191205	44.99	<0.001
R/L × R/L	1	0.01184	0.011841	2.79	0.139
PT × PT	1	0.20195	0.201945	47.51	<0.001
2-Way Interaction	1	0.39958	0.399582	94.01	<0.001
pH × R/L	1	0.39958	0.399582	94.01	<0.001
Error	7	0.02975	0.00425		
Lack-of-fit	5	0.02046	0.004092	0.88	0.608
Pure error	2	0.0093	0.004648		
Total	14	2.11081			
R^2		0.9859			
Adjusted R^2		0.9718			

[a] Degree of freedom.
[b] Some of squares.
[c] Mean of squares.

our model is very small (<0.001) which is an indication of significance of the obtained model. We then look at the values of R^2 and adjusted R^2 (see Table 3) which are both very close to unity and serve as another positive indication of the fitting quality of our model. To check the model adequacy, we calculate the lack-of-fit parameter. In our results, the F-value of the lack-of-fit is 0.88, which is very much less than the (critical) maximum value of 4, and the P-value is 0.608 which is higher than the (critical) minimum value of 0.05. These show that the lack-of-fit of our model is insignificant and that our model has an acceptable adequacy.

A final test for the accuracy of our model is the investigation of the residuals. We lay out normal probability plot and frequency versus residual respectively in Fig. 3(a) and (b). Near linear dependence of percent to residual and a bell-shaped frequency histogram shows that our residual has a normal distribution. We also plot residual as a function of the fitted value (Fig. 3(c)), and observation order (Fig. 3(d)). For a good quality fitting, both plots need to be random and not following any specific pattern. This is in fact seen in both plots and therefore our model successfully passes this last test.
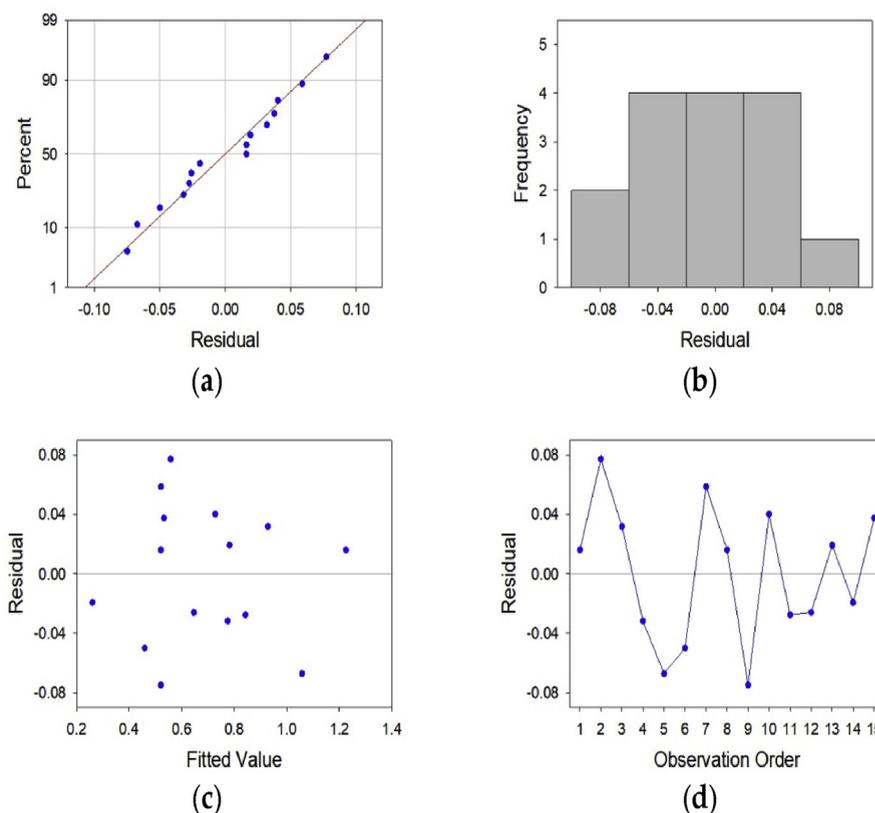
Fig. 3. Statistical graphs for evaluation of RSM full quadratic fitted model of Carbon Xerogel density: (a) Normal probability plot; (b) frequency versus residual plot; (c) residual versus fitted values plot and (d) residual versus observation order plot.

Now that our model is carefully checked for accuracy and quality of fitting, we plot response surfaces in order to investigate the effect of each of pH, R/L and PT on the density (Fig. 4, note that since there are three parameters affecting the density, we need to plot three separate surfaces). As Fig. 4(a) shows, decrease in the pH or R/L results in the decrease in density. For a given pH or R/L, the lowest density which is correspond to the highest porosity is obtained in the middle of the chosen range for PT (i.e. the minimum density is obtained for a $600 < PT_{cr} < 900$; Fig. 4(b) and (c)).

The global minimum of density for the chosen range is $\rho = 0.26$ g/cm^3 which is obtained for pH $= 5.5$, R/L $= 30\%$ and PT $= 727.3$ (see Fig. 5). This global minimum is less sensitive to PT when compared to the effect of pH and R/L as can be seen from the slope of the optimization curves in Fig. 5. For verification of these findings, we run an experiment (repeated three times) with the optimum values of pH, R/L and PT reported above. The density we obtained is within 4% of the theoretical density reported above.

The optimum density we arrived at (i.e. $\rho = 0.26$) is quite competitive with the density of Carbon gels synthesized via other methods reported in the literature. For
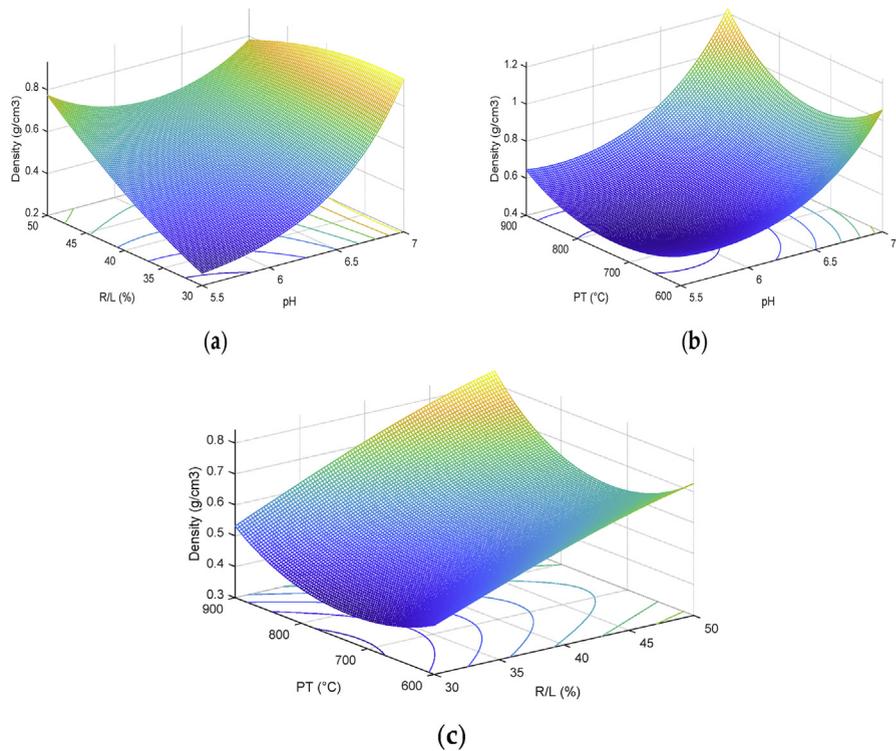
Fig. 4. Surface plots of target density versus different variables: (a) pH and R/L (hold value: PT = 750); (b) pH and PT (hold value: R/L = 40) and (c) R/L and PT (hold value: pH = 6.25).
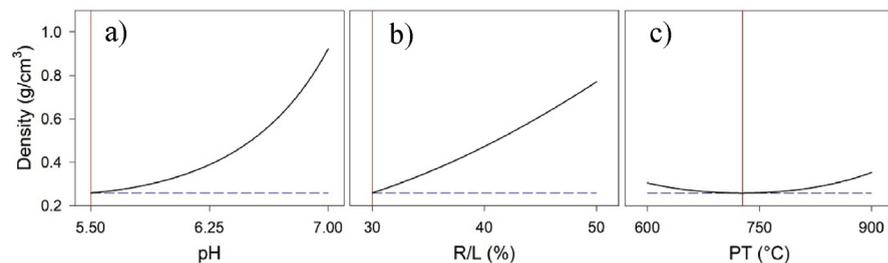

Fig. 5. Optimization plots for minimizing the density of final Carbon Xerogel catalyzed by NaOH: a) Density vs pH, b) Density vs R/L and c) Density vs PT.

instance, Jung et al. obtained a density of $\rho = 0.5$ g/cm^3 with the typical drying method at the ambient pressure and temperature [11], or Fu et al. obtained an optimum density of $\rho = 0.23$ g/cm^3 through supercritical drying in Isopropanol [50].

Positive slopes of the curve of density vs pH and R/L at the minimum values of pH and R/L suggests that with an even smaller values of pH and R/L a lower density may be achieved. This is not correct, because if R/L drops below 30%, the amount of reactants in the sample is too low for any gel structure to form. If pH drops below 5.5, the added catalyst to the initial RFC solution is very low and as a result curing or

gelation time will be very long and therefore the production of Carbon Xerogel is not economic and hence unjustifiable.

3.3. Capacitance maximization of Carbon Xerogel using Response Surface Methodology (RSM)

It is expected that the optimum synthesized sample with the minimum density (i.e. maximum porosity) has the maximum capacitance. To experimentally verify this, we measure the capacitance of each of our 15 samples via Cyclic Voltammetry method. Values of the capacitance of the samples are provided in Table 2. We again use the RSM to find the best fitted model for the capacitance vs our three parameters of pH, R/L and PT given in coded and actual values as Eqs. (7) and (8) respectively.

$$Y = 31.955 - 3.695X_1 + 1.685X_2 + 5.443X_3 - 7.894X_1^2 - 15.606X_3^2$$
$$+ 6.611X_1X_2 - 6.367X_1X_3, \qquad (7)$$

$$Capacitance = -954.5 + 177.7\,pH + 5.340\,R/L + 1.4304\,PT - 14.03\,pH^2$$
$$- 0.000694\,PT^2 + 0.881\,pH \times R/L - 0.05659\,pH \times PT. \qquad (8)$$

As before, we need to check the quality and adequacy of our model. Here, the P-value < 0.001 and therefore the model is significant; $R^2 = 98.88$ and adjusted $R^2 = 97.76$ and therefore the model has a good fitting quality; and the lack-of-fit parameter has a P-value of 0.902 and F-value of 0.26 (Table 4) and therefore the lack-of-fit parameter is insignificant.

Normal probability plot of residuals and histogram of frequency is shown respectively in Fig. 6(a) and (b). These two show that the residuals follow a normal distribution. We also plot residuals vs fitted values (Fig. 6(c)) and residuals as a function of observation order (Fig. 6(d)). Randomness of the data in these two plots show that the model fits the data well and the test sequence of experiments has no effect on the results.

Response surface curves for the target parameter (i.e. capacitance) show that for a high pH, an increase in R/L enhances the capacitance (Fig. 7(a)). This trend is reversed for low values of pH. As suggested by Fig. 7(c), for a moderate pH, R/L and PT are nearly independent.

The optimum capacitance is obtained for an optimal values of pH and PT within the chosen domain (the optimal pH value is close to the beginning of the domain), and for an optimal value of R/L which is at the boundary (minimum) of the selected domain (Fig. 7). These can be seen clearly in optimization plots of Fig. 8. Slopes of these curves suggest that the capacitance is a strong function of pH and PT, while it is not very much affected by the R/L. In other words, the capacitance is sensitive to pH and PT, but not very much to R/L. The maximum capacitance predicted by RSM

Table 4. ANOVA table of RSM represented model for Capacitance.

Source	DF[a]	Adj SS[b]	Adj MS[c]	F-value	P-value
Model	7	2.08106	0.297294	69.95	<0.001
Linear	3	368.96	122.987	42.58	<0.001
pH	1	109.23	109.229	37.82	<0.001
R/L	1	22.73	22.726	7.87	0.026
PT	1	237.01	237.005	82.05	<0.001
Square	2	1076.19	538.095	186.29	<0.001
pH × pH	1	231.43	231.429	80.12	<0.001
R/L × R/L	1	904.64	904.636	313.19	<0.001
PT × PT	2	336.95	168.475	58.33	<0.001
2-Way interaction	1	174.8	174.804	60.52	<0.001
pH × R/L	1	162.15	162.147	56.14	<0.001
Error	7	20.22	2.888		
Lack-of-fit	5	7.99	1.599	0.26	0.902
Pure error	2	12.22	6.112		
Total	14	1802.32			

R^2		0.9888			
Adjusted R^2		0.9776			

[a] Degree of freedom.
[b] Some of squares.
[c] Mean of squares.

is 35.3 F/g, obtained for optimal values of pH = 5.7, R/L = 30% and PT = 800. We then experimentally synthesize a sample with these optimal values and measured the capacitance of the obtained sample which shows the value of 37.6 F/g. The slope of the capacitance vs R/L curve is negative at the beginning of the domain, which suggests that for lower values of R/L a higher capacitance can be obtained. But as discussed before, for lower R/L ratios, gel cannot structurally formed. In other words, we practically do not get any gels for lower ratios of R/L. Closeness of the optimal values for maximizing the capacitance (pH = 5.7, R/L = 30%, PT = 800) and optimal values for minimizing the density (pH = 5.5, R/L = 30%, PT = 730) supports our hypothesis of the effect of porosity on the capacitance.

It is to be noted that higher ion absorption is correlated with higher porosity under the condition that the solution can permeate throughout our sample. In other words, contribution of porosity of an electrode is very little if inner pores are not connected to the surface of the electrode. In this case clearly the solution cannot get into inner pores and therefore inner pores do not play any role in the ion absorption. In an ideal case, we expect the nano-size inner pores to be connected to the surface of our electrode via micro-size channels (connected micro-pores). Therefore, the distribution of
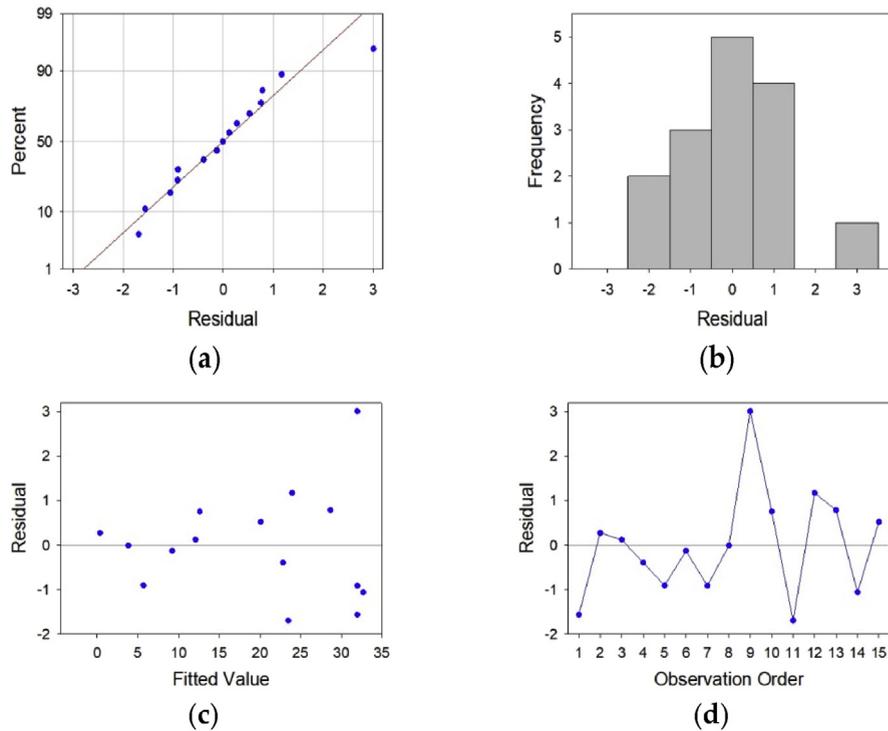
Fig. 6. Statistical graphs for evaluation of RSM full quadratic fitted model of Carbon Xerogel capacitance: (a) Normal probability plot; (b) frequency versus residual plot; (c) residual versus fitted values plot and (d) residual versus observation order plot.
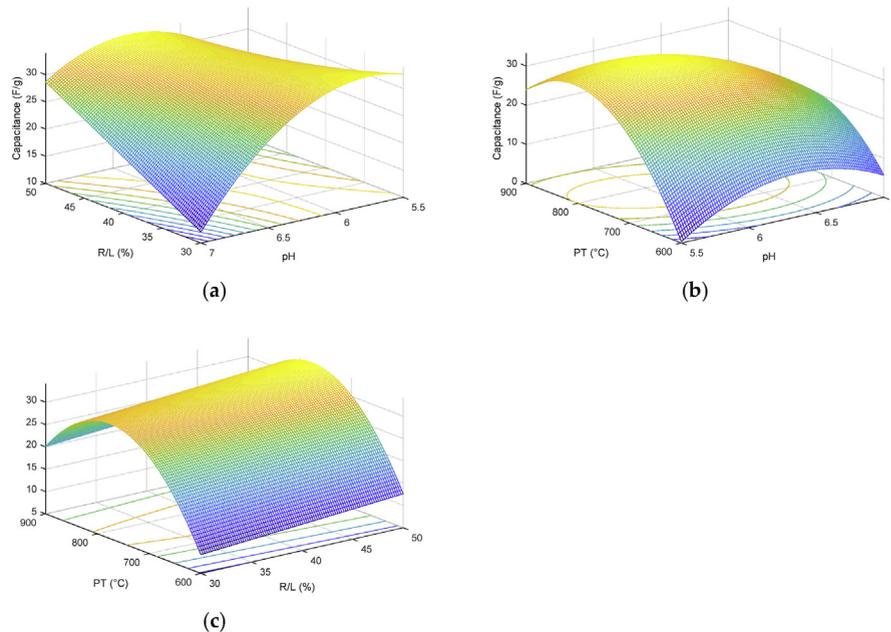

Fig. 7. Surface plots of target capacitance versus different variables: (a) pH and R/L (hold value: PT = 750); (b) pH and PT (hold value: R/L = 40) and (c) R/L and PT (hold value: pH = 6.25).
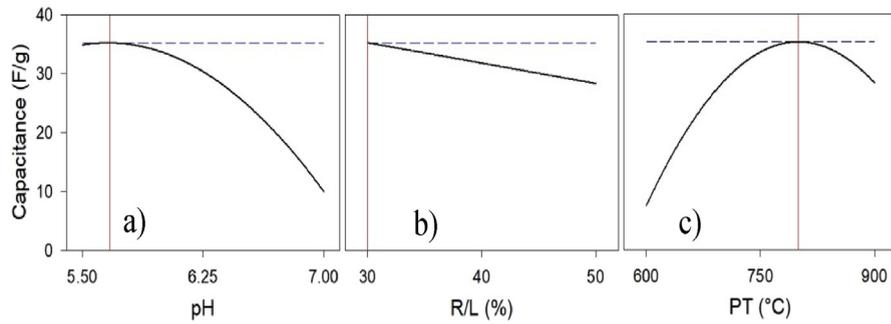
Fig. 8. Optimization plots for maximizing the capacitance of final Carbon Xerogel catalyzed by NaOH: a) Capacitance vs pH, b) Capacitance vs R/L and c) Capacitance vs PT.

pore sizes and their connectivity are also important to achieve the maximum gravimetric capacitance.

The size and distribution of pores in our optimized Carbon Xerogel is shown in Fig. 9 through SEM images. As shown in these images, the final electrode has a
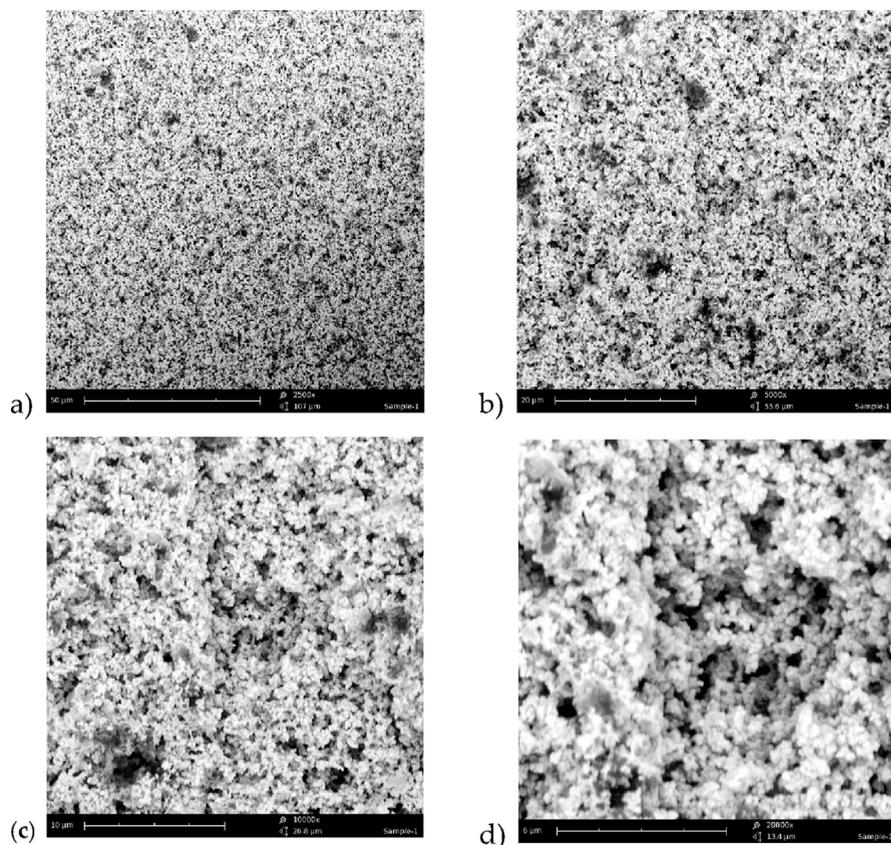

Fig. 9. The SEM images of our final optimized Carbon Xerogel in different zoom levels: a) 2500×, b) 5000×, c) 10000× and d) 20000×.
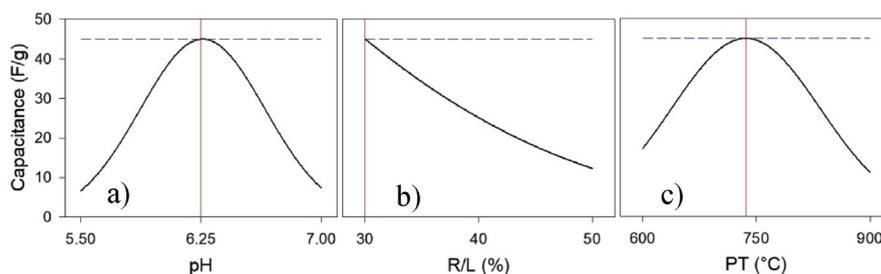
Fig. 10. Optimization plots for maximizing the capacitance of final Carbon Xerogel catalyzed by Na_2CO_3: a) Capacitance vs pH, b) Capacitance vs R/L and c) Capacitance vs PT [51].

uniform structure and the combination of Micro- and Nano-sized pores provides a very good condition for its ion adsorption capacitance (electrochemical capacitance).

Finally, we would like to comment on the effect of the catalyst on the capacitance of the final Carbon Xerogel. To do so, we compare the results of the synthesis with NaOH versus Na_2CO_3 as the catalyst under otherwise similar conditions (Figs. 8 and 10). Traditionally, and as discussed before, some researchers believed that, only the pH of the initial RFC (and not the catalyst type) is the main factor influencing the capacitance [19, 20]. However, comparing optimization curves for Carbon Xerogel synthesized with NaOH and Na_2CO_3 catalysts, it is clearly seen that with the same pH, extremely different capacitances are obtained. Specifically, in our experiment and under a chosen set of parameters: pH = 5.5, R/L = 30% and PT = 750 °C, NaOH catalyst gives a capacitance of 31.63 F/g and Na_2CO_3 leads to a capacitance of 6.49 F/g. A further investigation of different catalysts release that the highest capacitance with NaOH as the catalyst is obtained at pH = 5.7 and is equal to 37.6 F/g, and with Na_2CO_3 is obtained at pH = 6.25 and is equal to 42.3 F/g. As it can be seen from the optimization curves, the effect of R/L and PT on the capacitance follows a similar trend (Figs. 8 and 10).

4. Conclusions

In this study, we use a multi-parameter optimization to maximize the capacitance of Carbon Xerogel. The objective is to enhance the performance of Carbon Xerogel while maintaining its simple and economic synthesis process, hence the low production cost. We consider the effect of pH, R/L (Reactance to Liquid mass ratio) and PT (Pyrolysis Temperature), which are the most important parameters, on the capacitance and density of the final Carbon Xerogel, and as the catalyst, we select NaOH which is widely available. Through an optimization via Response Surface Methodology (RSM), we showed that with pH = 5.5, R/L = 30% and PT = 730, a Carbon Xerogel with the minimum density of 0.26 g/cm^3; and with pH = 5.7, R/L = 30% and PT = 800, a Carbon Xerogel with a maximum capacitance of 37.6 F/g is obtained. Closeness of optimal values of pH, R/L and PT for the

minimum density and maximum capacitance supports the hypothesis that porosity is correlated with the gravimetric capacitance. We also showed that — contrary to what is suggested in some literature- even with the same pH, the type of the catalyst can significantly affect the final capacitance of the Carbon Xerogel. Specifically, here we considered and compared similar samples at the same initial pH, but with NaOH and Na_2CO_3 as the catalyst and showed that an extremely difference of about 80% in capacitance is resulted. The maximum capacitance with $NaOH/Na_2CO_3$ as the catalyst is obtained at pH = 5.7/pH = 6.25 and is equal to c = 37.6/c = 42.3 F/g. It is hoped that our results paves the path for a more economic and with higher performance electrode production particularly for supercapacitors and CDI system.

Declarations

Author contribution statement

Mahdi Alam: Conceived and designed the experiments; Performed the experiments; Analyzed and interpreted the data; Contributed reagents, materials, analysis tools or data; Wrote the paper.

Seyed A. Mirbagheri: Analyzed and interpreted the data; Contributed reagents, materials, analysis tools or data; Wrote the paper.

Mohammad R. Ghaani: Conceived and designed the experiments; Analyzed and interpreted the data.

Funding statement

Competing interest statement

The authors declare no conflict of interest.

Additional information

No additional information is available for this paper.

References

[1] A.G. Pandolfo, A.F. Hollenkamp, Carbon properties and their role in supercapacitors, J. Power Sources 157 (2006) 11−27.

[2] A. González, E. Goikolea, J.A. Barrena, R. Mysyk, Review on supercapacitors: technologies and materials, Renew. Sustain. Energy Rev. 58 (2016) 1189−1206.

[3] K. Shi, I. Zhitomirsky, Influence of chemical structure of dyes on capacitive dye removal from solutions, Electrochim. Acta 174 (2015) 588−595.

[4] Z.-H. Huang, Z. Yang, F. Kang, M. Inagaki, Carbon electrodes for capacitive deionization, J. Mater. Chem. A 5 (2017) 470−496.

[5] J. Oladunni, J. Zain, A. Hai, F. Banat, G. Bharath, E. Alhseinat, A comprehensive review on recently developed carbon based nanocomposites for capacitive deionization : from theory to practice, Sep. Purif. Technol. 207 (2018) 291−320.

[6] K. Zaid, A.B. Suriani, A review on electrode materials used in capacitive deionization processes for water treatment applications, Sci. Int. 29 (2017) 285−289.

[7] S.-M. Chen, R. Ramachandran, V. Mani, R. Saraswathi, Recent advancements in electrode materials for the high-performance electrochemical supercapacitors: a review, Int. J. Electrochem. Sci. 9 (2014) 4072−4085.

[8] S. Mezzavilla, C. Zanella, C. Della, V. Gian, D. Soraru, Carbon xerogels as electrodes for supercapacitors. The influence of the catalyst concentration on the microstructure and on the electrochemical properties, J. Mater. Sci. 47 (2012) 7175−7180.

[9] L.L. Zhang, Carbon-Based Materials as Supercapacitor Electrodes, 2010.

[10] K. Shi, M. Ren, I. Zhitomirsky, Activated carbon-coated carbon nanotubes for energy storage in supercapacitors and capacitive water purification, Sustain. Chem. Eng. 2 (2014) 1289−1298.

[11] H.H. Jung, S.W. Hwang, S.H. Hyun, K.H. Lee, G.T. Kim, Capacitive deionization characteristics of nanostructured carbon aerogel electrodes synthesized via ambient drying, Desalination 216 (2007) 377−385.

[12] R. Kumar, S.S. Gupta, S. Katiyar, V.K. Raman, K.S. Varigala, T. Pradeep, A. Sharma, Carbon aerogels through organo-inorganic co-assembly and their application in water desalination by capacitive deionization, Carbon N. Y. 99 (2016) 375−383.

[13] A.M. Elkhatat, S.A. Al-Muhtaseb, Advances in tailoring resorcinol-formaldehyde organic and carbon gels, Adv. Mater. 23 (2011) 2887−2903.

[14] S.A. Al-muhtaseb, J.A. Ritter, Preparation and properties of resorcinol-formaldehyde organic and carbon gels, Adv. Mater. (2003) 101−114.

[15] J. Biener, M. Stadermann, M. Suss, M. a. Worsley, M.M. Biener, K. a. Rose, T.F. Baumann, Advanced carbon aerogels for energy applications, Energy Environ. Sci. 4 (2011) 656.

[16] M.-F. Yan, L. Zhang, R. He, Z.-F. Liu, Synthesis and characterization of carbon aerogels with different catalysts, J. Porous Mater. (2015) 699−703.

[17] K. Hussaro, Preparation of activated carbon from palm oil shell by chemical activation with Na_2CO_3 and $ZnCl_2$ as imprenated agents for H_2S adsorption, Am. J. Environ. Sci. 10 (2014) 336−346.

[18] P.M. Eletskii, V.A. Yakovlev, V.B. Fenelonov, V.N. Parmon, Texture and adsorptive properties of microporous amorphous carbon materials prepared by the chemical activation of carbonized high-ash biomass, Kinet. Catal. 49 (2008) 708−719.

[19] N. Job, R. Pirard, J. Marien, J. Pirard, Porous carbon xerogels with texture tailored by pH control during sol − gel process, Carbon N. Y. 42 (2004) 619−628.

[20] C.S. Sharma, M.M. Kulkarni, A. Sharma, M. Madou, Synthesis of carbon xerogel particles and fractal-like structures, Chem. Eng. Sci. 64 (2009) 1536−1543.

[21] T. Yamamoto, T. Nishimura, T. Suzuki, H. Tamon, Control of mesoporosity of carbon gels prepared by sol − gel polycondensation and freeze drying, J. Non-Cryst. Solids 288 (2001) 46−55.

[22] J. Feng, J. Feng, C. Zhang, Shrinkage and pore structure in preparation of carbon aerogels, J. Sol-Gel Sci. Technol. 59 (2011) 371−380.

[23] Y. Feng, L. Ge, B. Jiang, L. Miao, T. Masaki, Reactant concentration and carbonization to the controllable fabrication of carbon aerogels, Mater. Sci. Forum 744 (2013) 20−23.

[24] J. Li, X. Wang, J. Li, Q. Huang, X. Wang, S. Gamboa, Q. Huang, S. Gamboa, P.J. Sebastian, P.J. Sebastian, Studies on preparation and performances of carbon aerogel electrodes for the application of supercapacitor, J. Power Sources 158 (2006) 784.

[25] C. Macías, P. Lavela, G. Rasines, M.C. Zafra, J.L. Tirado, C.O. Ania, On the correlation between the porous structure and the electrochemical response of powdered and monolithic carbon aerogels as electrodes for capacitive deionization, J. Solid State Chem. 242 (2016) 21−28.

[26] J. Landon, X. Gao, B. Kulengowski, J.K. Neathery, K. Liu, Impact of pore size characteristics on the electrosorption capacity of carbon xerogel electrodes for capacitive deionization, J. Electrochem. Soc. 159 (2012) A1861−A1866.

[27] R. Saliger, V. Bock, R. Petricevic, T. Tillotson, S. Geis, J. Fricke, Carbon aerogels from dilute catalysis of resorcinol with formaldehyde, J. Non-Cryst. Solids 221 (1997) 144−150.

[28] W.E.I. Liu, A. Herrmann, N.C. Bigall, P. Rodriguez, D. Wen, M. Oezaslan, T.J. Schmidt, N. Gaponik, A. Eychmüller, Noble metal aerogels — synthesis, characterization , and application as electrocatalysts, Acc. Chem. Res. 48 (2015) 154−162.

[29] A. Halama, B. Szubzda, G. Pasciak, Carbon aerogels as electrode material for electrical double layer supercapacitors − synthesis and properties, Electro-chim. Acta 55 (2010) 7501−7505.

[30] N. Job, A. Théry, R. Pirard, J. Marien, L. Kocon, J.N. Rouzaud, F. Béguin, J.P. Pirard, Carbon aerogels, cryogels and xerogels: influence of the drying method on the textural properties of porous carbon materials, Carbon N. Y. 43 (2005) 2481−2494.

[31] C.A. García-González, M.C. Camino-Rey, M. Alnaief, C. Zetzl, I. Smirnova, Supercritical drying of aerogels using CO_2: effect of extraction time on the end material textural properties, J. Supercrit. Fluids 66 (2012) 297−306.

[32] D. Wu, R. Fu, M.S. Dresselhaus, G. Dresselhaus, Fabrication and nano-structure control of carbon aerogels via a microemulsion-templated sol − gel polymerization method, Carbon N. Y. 44 (2006) 675−681.

[33] B. Babić, B. Kaluderović, L. Vračar, N. Krstajić, Characterization of carbon cryogel synthesized by sol-gel polycondensation and freeze-drying, Carbon N. Y. 42 (2004) 2617−2624.

[34] H. Tamon, H. Ishizaka, T. Yamamoto, T. Suzuki, Influence of freeze-drying conditions on the mesoporosity of organic gels as carbon precursors, Carbon N. Y. 38 (2000) 1099−1105.

[35] D.K. Kohli, S. Bhartiya, A. Singh, R. Singh, M.K. Singh, P.K. Gupta, Capac-itive deionization of ground water using carbon aerogel based electrodes, De-salin. Water Treat. 3994 (2016) 1−9.

[36] H. Pröbstle, M. Wiener, J. Fricke, Carbon aerogels for electrochemical double layer capacitors, J. Porous Mater. 10 (2003) 213−222.

[37] B. Fang, L. Binder, A modified activated carbon aerogel for high-energy stor-age in electric double layer capacitors, J. Power Sources 163 (2006) 616−622.

[38] B. Jia, W. Zhang, Preparation and application of electrodes in capacitive deionization (CDI): a state-of-art review, Nanoscale Res. Lett. 11 (2016) 64.

[39] S. Chandrasekaran, P.G. Campbell, T.F. Baumann, M.A. Worsley, Carbon aerogel evolution: allotrope, graphene-inspired, and 3D-printed aerogels, J. Mater. Res. (2017) 1−20.

[40] M.R. Ghaani, P. Marashi, L16 orthogonal design synthesis of NASICON-type Li1.4Al0.4Ti1.6(PO4)3 solid electrolyte by pechini method for process optimization, Iran, J. Mater. Sci. Eng. 15 (2018) 60−71.

[41] J. Liu, Z. Xiong, S. Wang, W. Cai, J. Yang, H. Zhang, Structure and electrochemistry comparison of electrospun porous carbon nanofibers for capacitive deionization, Electrochim. Acta 210 (2016) 171−180.

[42] S. Porada, R. Zhao, A. van der Wal, V. Presser, P.M. Biesheuvel, Review on the science and technology of water desalination by capacitive deionization, Prog. Mater. Sci. 58 (2013) 1388−1442.

[43] E. García-Quismondo, C. Santos, J. Soria, J. Palma, M.A. Anderson, New operational modes to increase energy efficiency in capacitive deionization systems, Environ. Sci. Technol. 50 (2016) 6053−6060.

[44] Z. Zapata-Benabithe, F. Carrasco-Marin, C. Moreno-Castilla, Preparation, surface characteristics, and electrochemical double-layer capacitance of KOH-activated carbon aerogels and their O- and N-doped derivatives, J. Power Sources 219 (2012) 80−88.

[45] Y.C. Tsai, R. an Doong, Hierarchically ordered mesoporous carbons and silver nanoparticles as asymmetric electrodes for highly efficient capacitive deionization, Desalination 398 (2016) 171−179.

[46] D. Wu, X. Chen, S. Lu, Y. Liang, F. Xu, R. Fu, Microporous and mesoporous materials study on synergistic effect of ordered mesoporous carbon and carbon aerogel during electrochemical charge−discharge process, Microporous Mesoporous Mater. 131 (2010) 261−264.

[47] S. Kim, J. Lee, C. Kim, J. Yoon, Na$_2$FeP$_2$O$_7$ as a novel material for hybrid capacitive deionization, Electrochim. Acta 203 (2016) 265−271.

[48] G. Wang, C. Pan, L. Wang, Q. Dong, C. Yu, Z. Zhao, J. Qiu, Activated carbon nanofiber webs made by electrospinning for capacitive deionization, Electrochim. Acta 69 (2012) 65−70.

[49] K. Laxman, M.T.Z. Myint, M. Al Abri, P. Sathe, S. Dobretsov, J. Dutta, Desalination and disinfection of inland brackish ground water in a capacitive

deionization cell using nanoporous activated carbon cloth electrodes, Desalination 362 (2015) 126−132.

[50] R. Fu, B. Zheng, J. Liu, S. Weiss, J.Y. Ying, M.S. Dresselhaus, G. Dresselhaus, J.H. Satcher, T.F. Baumann, Studies of the chemical and pore structures of the carbon aerogels synthesized by gelation and supercritical drying in isopropanol, J. Appl. Polym. Sci. 91 (2004) 3060−3067.

[51] M. Alam, S.A. Sadrnejad, M.R. Ghaani, Performance evaluation of optimized carbon xerogel electrode in desalination through flow-electrode capacitive deionization: capacitance optimization by response surface methodology, Desalin. Water Treat. (2019) (In press).